Chapter 6

Overview of Membrane Protein Purification and Crystallization

Tatsuro Shimamura

Abstract

The three-dimensional structures of proteins provide important information for elucidation of the mechanisms and functions of the proteins. However, membrane proteins are difficult to crystallize and available structural information on membrane proteins is very limited. The difficulty is mainly due to the hydrophobic nature and the instability of membrane proteins, which increase some parameters in their purification and crystallization procedures. Recently, some new techniques such as the antibody technique and the lipidic cubic phase crystallization technique were applied to the production of high-quality crystals of membrane proteins. In this chapter, the protocols for the purification of the membrane protein and the lipidic cubic phase crystallization technique are described.

Keywords Membrane protein, Lipidic cubic phase, Crystallization, Detergent, In meso, Antibody

1 Introduction

Approximately 30 % of proteins encoded in the human genome are membrane proteins [1, 2]. They are involved in a variety of essential biological functions such as signal transduction, solute transport, and energy conversion. Despite their essential roles, membrane proteins are known to be difficult to crystallize compared with soluble proteins. Actually, of nearly 120,000 entries in the Protein Data Bank (PDB) [3], only around 610 structures are of unique integral membrane proteins [4]. The difficulty is mainly due to the hydrophobic nature and the instability of membrane proteins, which increase some parameters in the purification and crystallization procedures of membrane proteins [5, 6].

Membrane proteins are embedded within the lipid bilayer and very insoluble. The first step of the purification process is thus to solubilize the membrane protein from the membrane using detergent. Detergent molecules are amphiphilic with a polar head and a hydrophobic tail. At lower concentrations, the detergent molecules exist as monomers in aqueous solution. At the critical micelle

Toshiya Senda and Katsumi Maenaka (eds.), *Advanced Methods in Structural Biology*, Springer Protocols Handbooks,
DOI 10.1007/978-4-431-56030-2_6, © Springer Japan 2016

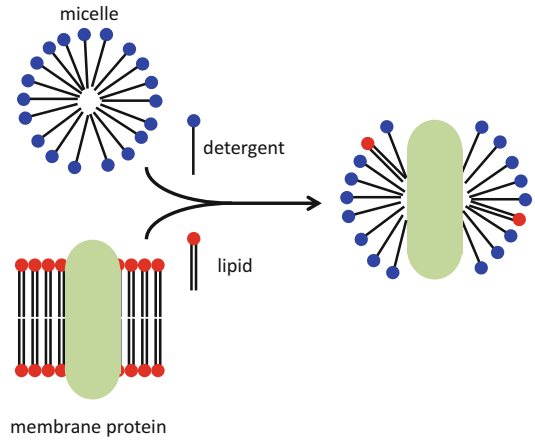

Fig. 1 Solubilization of membrane proteins

concentration (CMC), the detergent molecules begin to self-associate and form micelles [7]. When added to the membrane, the detergent molecules disrupt the membrane structure and cover the hydrophobic surface of the membrane protein, generating water-soluble protein-detergent micelles (Fig. 1). Nonionic sugar detergents such as maltosides and glucosides are most often used for membrane protein purification and crystallization (Table 1). The recently developed maltose neopentyl glycol (MNG) amphiphiles have shown effectively to stabilize several membrane proteins compared with conventional detergents, leading to successful crystallization [8–11]. Using these mild detergents, the membrane proteins are extracted from the membrane in their native conformation. Generally the concentration of the detergent required for the solubilization of membrane proteins is much higher than the CMC. For example, n-dodecyl-β-D-maltoside (DDM), one of the most popular sugar detergents whose CMC is ~0.0087 % (Table 1) in water, is used for solubilization at a concentration of 0.5–1 %. The concentration of the detergent can be decreased to two to three times higher than the CMC at later steps in the purification procedure. The detergent used for solubilization does not need to be the same as the detergent in the later steps of the purification and crystallization; it can be exchanged for another detergent during purification.

Except for solubilization, the purification procedures for membrane proteins are essentially the same as those for soluble proteins. Immobilized metal affinity chromatography (IMAC) is an efficient and high-speed method for the purification of membrane proteins [12, 13]. Cleavage of the affinity tag from the protein increases the likelihood of crystallization. The presence of detergent molecules may decrease the efficiency of proteolysis by blocking the access of the protease to the cleavage site or by inhibiting the protease

Table 1
Common detergents

	M_r	CMC[a]
Nonionic		
Glucosides or maltosides		
n-Octyl-β-D-glucoside	292.4	18–20 mM (0.53 %)
n-Nonyl-β-D-glucoside	306.4	6.5 mM (0.20 %)
n-Decyl-β-D-glucoside	320.4	2.2 mM (0.0070 %)
n-Nonyl-β-D-maltoside	468.5	6 mM (0.28 %)
n-Decyl-β-D-maltoside	482.6	1.8 mM (0.087 %)
n-Undecyl-β-D-maltoside	496.6	0.59 mM (0.029 %)
n-Dodecyl-β-D-maltoside	510.6	0.17 mM (0.0087 %)
n-Tridecyl-β-D-maltoside	524.6	0.033 mM (0.0017 %)
n-Octyl-β-D-thioglucoside	308.4	9.0 mM (0.28 %)
n-Nonyl-β-D-thioglucoside	322.4	2.9 mM (0.093 %)
n-Octyl-β-D-thiomaltoside	470.6	8.5 mM (0.4 %)
n-Nonyl-β-D-thiomaltoside	484.6	3.2 mM (0.15 %)
n-Decyl-β-D-thiomaltoside	498.6	0.9 mM (0.045 %)
n-Undecyl-β-D-thiomaltoside	512.7	0.21 mM (0.011 %)
n-Dodecyl-β-D-thiomaltoside	526.6	0.05 mM (0.0026 %)
CYGLU-4	318.4	1.8 mM (0.058 %)
CYMAL-5	494.5	2.4 mM (0.12 %)
CYMAL-6	508.5	0.56 mM (0.028 %)
CYMAL-7	522.5	0.19 % (0.0099 %)
Octyl glucose neopentyl glycol	569.7	1.02 mM (0.058 %)
Decyl maltose neopentyl glycol	949.1	0.036 mM (0.0034 %)
Lauryl maltose neopentyl glycol	1005.2	0.01 mM (0.001 %)
Polyoxyethylene glycols		
C8E4	306.5	8 mM (0.25 %)
C10E5	378.6	0.81 mM (0.031 %)
C10E6	423.0	0.9 mM (0.038 %)
C12E8	538.8	0.09 mM (0.0048 %)
C12E9	583.0	0.05 mM (0.003 %)
Triton X-100	avg. 647	0.23 mM (0.015 %)

(continued)

Table 1
(continued)

	M_r	CMC[a]
Zwitterionic detergents		
CHAPS	614.9	8 mM (0.49 %)
LDAO	229.4	1–2 mM (0.023 %)

[a]CMC values were from the Affymetrix Anatrace Products catalog [46]

activity [14]. These can be sometimes avoided by increasing the amount of protease, or by changing the location of the tag, or by inserting few hydrophilic amino acid residues between the protein and the tag to expose the cleavage site to the protease. Other chromatographic techniques such as size-exclusion chromatography and ion-exchange chromatography are also available. It should be remembered that the membrane proteins are covered by detergent molecules, which expands the hydrodynamic radius of the protein. Moreover, the membrane protein-detergent micelles tend to interact strongly with the chromatography matrix, lowering the column efficiency. The purity should be as high as possible but overpurification sometimes loses structural components such as subunits of membrane protein complexes or lipids [15]. Homogeneity of the purified protein can be assessed using size-exclusion chromatography. Monodispersity is a critical prerequisite for successful crystallization.

Once sufficient amounts (at least ~0.5 mg) of the membrane protein have been obtained with high purity and monodispersity, one can try to crystallize the protein. Membrane protein three-dimensional (3D) crystals are classified into two types, type I and type II (Fig. 2) [5, 6]. Type I crystals are built by stacks of two-dimensional (2D) crystals. The crystals formed in a lipidic cubic phase (LCP) belong to type I. Type II crystals are obtained using the standard crystallization methods routinely applied to soluble proteins, and most membrane crystals belong to this type. In type II crystals, only the hydrophilic surfaces of the membrane protein can be involved in the rigid crystal contacts. Therefore, the membrane proteins with small hydrophilic surfaces are especially difficult to crystallize. Moreover, the detergent molecules covering the hydrophobic surfaces need space in the crystal lattice, meaning that the crystals have a very high solvent content (65–80 %) and diffract poorly. These issues can be overcome in several ways [5, 6]. Firstly, the shorter alkyl chain detergents generally form smaller micelles, producing more surface area for the crystal contacts. It is recommended to solubilize the membrane protein using a longer chain detergent and exchange it for a shorter chain detergent. This is because the shorter chain detergent generally has a larger CMC

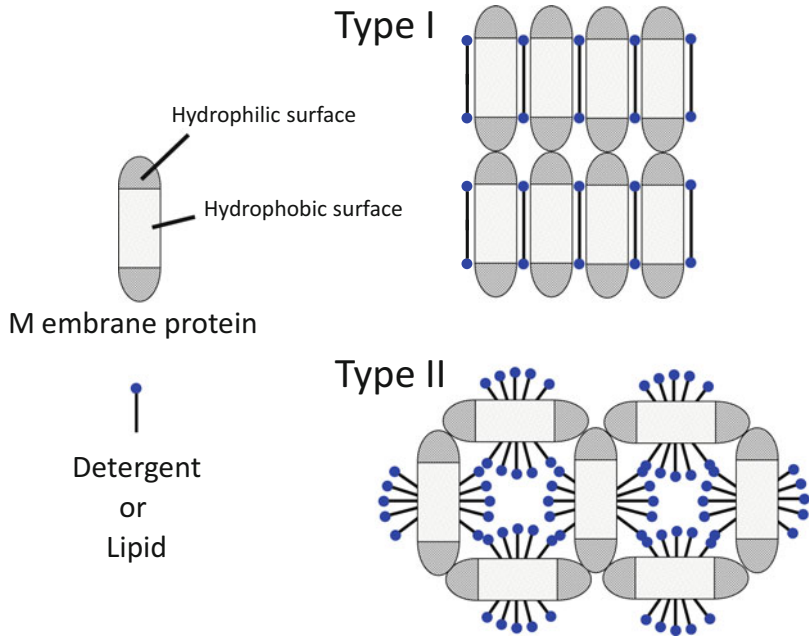

Fig. 2 Basic types of membrane protein 3D crystals

and is required at a higher concentration for solubilization, although the longer chain detergent with very low CMC is difficult to replace completely with the shorter chain detergent. In the case of the crystallographic study of Mhp1, a hydantoin transporter, DDM was used for solubilization and exchanged for n-nonyl-β-D-maltoside at the Ni-affinity chromatography step by washing extensively with buffer containing the detergent, which was essential for the successful crystallization of Mhp1 [16–18]. However, it should be noted that membrane proteins are less stable when covered by a shorter chain detergent. The use of the thermostabilized mutant is sometimes effective to overcome the instability as was shown in the structural study of the turkey β_1 adrenergic receptor [19]. The second way to reduce the micelle size is the addition of small amphiphilic molecules. For example, the addition of 5 % 1,2,3-heptanetriol has shown to reduce the number of *N*,*N*-Dimethyldodecylamine *N*-oxide (LDAO) associated with the reaction center from *Rhodopseudomonas viridis* [20]. The third way is to expand the hydrophilic surface by the specific binding of a soluble protein. As the soluble protein, antibody (Fv fragment, Fab fragment, nanobody), DARPin (designed ankyrin repeat protein) [21] and monobody (fibronectin type III domain) [22] have been used so far for crystallization. The antibody technique was first applied to crystallographic studies of cytochrome *c* oxidase (Fig. 3a, b) [23–25] and has been successfully used for the structure determination of several membrane proteins such as the cytochrome bc_1 complex [26], the KcsA potassium channel [27],

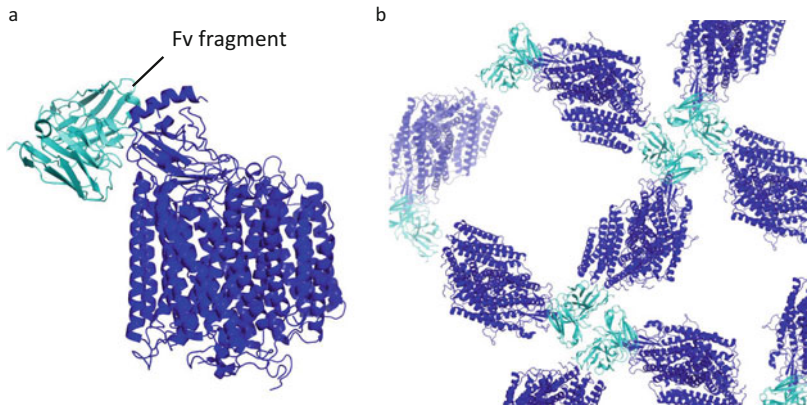

Fig. 3 Fv fragment essential for the crystallization of cytochrome *c* oxidase. (**a**) Structure of cytochrome *c* oxidase-Fv complex. Cytochrome *c* oxidase is shown in *blue* and Fv fragment *cyan*. (**b**) Crystal packing of cytochrome *c* oxidase-Fv complex

and adenosine A_{2a} receptor [28]. In the case of adenosine A_{2a} receptor, the Fab fragment recognizes the 3D structure of the receptor and contributes not only to the expansion of the hydrophilic area but also to the stabilization of the inactive conformation. Nanobody is a small single chain antibody of a llama and was used for structure determinations of the active conformation of G protein-coupled receptors [9, 29, 30].

Crystallization in lipidic mesophase (also known as LCP crystallization or *in meso* crystallization) has been successfully used to determine the high-resolution structures of membrane proteins since it was first applied to the crystallization of bacteriorhodopsin [31]. The first step of the technique is to reconstitute the purified membrane protein in the lipid bilayer prepared by mixing aqueous buffer with lipids such as monoolein under appropriate conditions. Addition of salts and precipitants may produce tiny crystals in LCP. The LCP technique has several advantages compared with the crystallization technique in detergent micelles. First, the membrane protein is more stable in a more native-like environment [32]. Second, the crystals in LCP belong to type I and crystal contacts are established by the hydrophobic surface as well as the hydrophilic surface of the protein, resulting in lower solvent content and higher crystal quality [33]. However, the LCP technique has some disadvantages. The crystals in LCP are generally very tiny and difficult to detect. Moreover, the curved nature of the lipid membrane and the specific microstructure sets a limit to the size of membrane proteins to be crystallized [34]. This obstacle can be overcome by the use of specific precipitants, such as nonvolatile alcohols, small PEGs, etc., that swell and transform LCP to a sponge phase [34–36] or special lipids that enlarge the size of the water channel in LCP [9].

Here, protocols for the membrane protein purification and the LCP crystallization techniques are presented. These are essentially the same methods used for the crystallographic study of human histamine H_1 receptor [37, 38]. Other textbooks [5, 6], papers [39, 40], a web site [41], movies [42, 43], and manufacturer's manuals [44–46] also provide very useful information about these techniques.

2 Materials

1. Glass beads (0.5 mm diameter).
2. n-Dodecyl-β-D-maltoside (DDM).
3. Breaking buffer: 50 mM HEPES pH7.5, 120 mM NaCl, 5 % glycerol, 2 mM EDTA, and one tablet of protein inhibitor cocktail/50 ml.
4. Lysis buffer: 10 mM HEPES pH7.5, 10 mM $MgCl_2$, 20 mM KCl, and one tablet of protein inhibitor cocktail/50 ml.
5. High salt buffer: 10 mM HEPES pH7.5, 10 mM $MgCl_2$, 20 mM KCl, 1 M NaCl, and one tablet of protein inhibitor cocktail/50 ml.
6. Membrane buffer: 50 mM HEPES pH7.5, 120 mM NaCl, 20 % glycerol, and one tablet of protein inhibitor cocktail/50 ml.
7. Iodoacetamide.
8. Solubilization buffer: 50 mM HEPES pH7.5, 500 mM NaCl, 20 % glycerol, 1 % DDM, and one tablet of protein inhibitor cocktail/50 ml.
9. Imidazole.
10. Talon resin.
11. Talon wash buffer 1: 50 mM HEPES pH7.5, 500 mM NaCl, 10 % glycerol, 0.025 % DDM, 20 mM imidazole, 10 mM $MgCl_2$, 8 mM ATP, and one tablet of protein inhibitor cocktail/50 ml.
12. Talon wash buffer 2: 50 mM HEPES pH7.5, 500 mM NaCl, 10 % glycerol, 0.025 % DDM, 20 mM imidazole, and one tablet of protein inhibitor cocktail/50ml.
13. Talon elution buffer: 50 mM HEPES pH7.5, 500 mM NaCl, 10 % glycerol, 0.025 % DDM, 200 mM imidazole, and one tablet of protein inhibitor cocktail/50ml.
14. PD10 desalting column.
15. Ni-sepharose resin.

16. Ni-elute buffer: 20 mM HEPES pH7.5, 500 mM NaCl, 10 % glycerol, 0.025 % DDM, 400 mM imidazole, and one tablet of protein inhibitor cocktail/50 ml.
17. Reverse IMAC buffer: 50 mM HEPES pH7.5, 500 mM NaCl, 10 % glycerol, 0.025 % DDM, and one tablet of protein inhibitor cocktail/100 ml.
18. Ni-sepharose high-performance resin.
19. BCA protein assay kit.
20. Monoolein.
21. Crystallization screens.
22. 100 μl Hamilton gas-tight syringe.
23. Coupler.

3 Methods

3.1 Membrane Preparation from Pichia pastoris *(see Note 1)*

1. Harvest cells by centrifuging at 5000 *g* for 5 min at 4 °C.
2. Discard the supernatant.
3. Resuspend the cells in cold water. A paintbrush is helpful when resuspending the cells.
4. Harvest cells by centrifuging at 5000 *g* for 5 min at 4 °C.
5. Resuspend 20–25 g of cell pellets in 100 ml of the breaking buffer.
6. Take a 10 μl sample of the resuspension to check the cell disruption and store at 4 °C.
7. Transfer the resuspension to a 2 L flask.
8. Add 150 g of glass beads to the flask.
9. Place the flask on an incubator shaker and disrupt the cells by shaking at 350 rpm at 4 °C for ~2 h.
10. Take a 10 μl sample of the homogenate and check the cell disruption by comparing it with the sample from step 6 using a microscope. More than 90 % of cells should be disrupted.
11. Transfer the homogenate to clean centrifuge tubes chilled on ice.
12. Remove intact cells and particles by centrifugation at 2000 *g* for 20 min at 4 °C.
13. Transfer the supernatant to clean ultracentrifugation tubes chilled on ice.
14. Balance the tubes and ultracentrifuge the supernatant at 100,000 *g* for 30 min at 4 °C.
15. Discard the supernatant.

16. Resuspend the pellets in 100 ml of lysis buffer.
17. Transfer the suspension to ultracentrifugation tubes.
18. Ultracentrifuge the suspension at 100,000 *g* for 30 min at 4 °C.
19. Discard the supernatant.
20. Resuspend the pellets in 100 ml of the high salt buffer.
21. Transfer the suspension to ultracentrifugation tubes.
22. Ultracentrifuge the suspension at 100,000 *g* for 30 min at 4 °C.
23. Discard the supernatant.
24. Repeat steps 20–23. The resultant membrane pellets are used for the purification.

3.2 Solubilization of the Membrane Protein

1. Resuspend ~10 g of the membrane pellets in 25 ml of the membrane buffer.
2. Transfer the resuspension to a clean chilled dounce homogenizer.
3. Add iodoacetamide (10 mg/ml).
4. Dounce ~40 times on ice.
5. Transfer the resuspension to a clean chilled beaker.
6. Keep the beaker on ice for 30 min.
7. Pour 50 ml of the solubilization buffer into the membrane suspension and stir gently at 4 °C for ~2 h (See Note 2).
8. Transfer the solubilization mixture to ultracentrifugation tubes.
9. Ultracentrifuge the solubilization mixture at 100,000 *g* for 30 min at 4 °C to remove the unsolubilized material.
10. Pool the supernatant in a clean chilled beaker.

3.3 First Affinity Purification Using Talon Resin [45]

1. Add imidazole (final 5 mM) and NaCl (final 800 mM) in the supernatant from step 10 in 3.2.
2. Add 10 ml of Talon resin equilibrated with the Talon wash buffer 1.
3. Agitate the mixture with a magnetic stir bar at 4 °C for 3–12 h.
4. Collect the Talon resin in a 50 ml Falcon tube by repeating centrifugation at 800 g and discarding the supernatant at 4 °C.
5. Wash the Talon resin with 10 bed volumes of the Talon wash buffer 1. Add the Talon wash buffer 1 in the Falcon tubes and agitate gently on a rotary shaker at 4 °C.
6. Centrifuge at 800 *g* for 5 min at 4 °C.
7. Discard the supernatant.

8. Repeat steps 6–8 with 10 bed volumes of the Talon wash buffer 1.
9. Wash the resin with the Talon wash buffer 2. Repeat steps 6–8 with 5 bed volumes of the Talon wash buffer 2.
10. Add 30 ml of the Talon wash buffer 2 in the tube and resuspend by vortexing.
11. Load the resin into a 20 ml gravity-flow column with the bottom outlet capped.
12. Remove the bottom cap and allow the buffer to drain. Save flow-through for SDS-PAGE analysis.
13. Elute the His-tagged protein by loading 10 ml of the Talon elution buffer on the resin in the column.
14. Collect the eluate in a 15 ml disposable tube.
15. Repeat steps 14–15 ten times.
16. Analyze the fractions by SDS-PAGE.
17. Pool the fractions containing the His-tagged protein.
18. Concentrate to 2.5 ml with a 100 kDa molecular weight cutoff concentrator.

3.4 Remove Imidazole Using PD10 Column

1. Take off the top cap of the PD10 column and remove the storage solution.
2. Cut the sealed end of the column.
3. Equilibrate the column with ~30 ml of the Talon wash buffer 2.
4. Apply the 2.5 ml of the concentrated sample to the column.
5. Let the sample enter the packed bed completely and discard the flow-through.
6. Place a 15 ml tube under the column for sample collection.
7. Load the 3.5 ml of the Talon wash buffer 2 to the column.
8. Collect the eluate.

3.5 Second Affinity Purification Using Ni-Sepharose Resin [44]

1. Equilibrate 4 ml of Ni-NTA resin with ~20 ml of the Talon wash buffer 2.
2. Add 4 ml of the Ni-NTA resin to the eluate from step 8 in 3.4.
3. Gently agitate on a rotary shaker at 4 °C for 2–12 h.
4. Transfer the mixture to a 20 ml disposable column.
5. Wash the resin by applying 45 ml of the Talon wash buffer 2.
6. Elute the His-tagged protein by with 24 ml of the Ni-elute buffer.
7. Collect the eluate and analyze the fractions by SDS-PAGE.
8. Pool the fractions containing the His-tagged protein.

9. Concentrate to 2.5 ml with a 100 kDa molecular weight cutoff concentrator.

3.6 Remove Imidazole Using PD10 Column

1. Take off the top cap of the PD10 column and remove the storage solution.
2. Cut the sealed end of the column.
3. Equilibrate the column with ~30 ml of the reverse IMAC buffer.
4. Apply the 2.5 ml of the concentrated sample to the column.
5. Let the sample enter the packed bed completely and discard the flow-through.
6. Place a 15 ml tube under the column for sample collection.
7. Load the 3.5 ml of the reverse IMAC buffer to the column.
8. Collect the eluate.
9. To cleave off the GFP-His-tag of the protein, add appropriate amount of His-tagged TEV protease to the eluate and incubate overnight at 4 °C.

3.7 Reverse IMAC (Immobilized-Metal Affinity Chromatography)

1. Equilibrate 0.6 ml of the Ni-sepharose high-performance resin with 6 ml of the reverse IMAC buffer.
2. Pour 0.6 ml of the Ni-sepharose high-performance resin into a 10 ml column.
3. Apply the protein mixture from step 9 in 3.6 on the column.
4. Collect the flow-through fraction (see Note 3).
5. Apply 8 ml of the reverse IMAC buffer to the column.
6. Collect the flow-through and add to the fraction from step 4.
7. Determine the protein concentration using a BCA protein assay kit following the manufacturer's instructions.
8. Concentrate the purified protein to ~30 mg/ml with a 100 kDa molecular weight cutoff concentrator.
9. Check the purity and monodispersity of the purified sample by SDS-PAGE and size-exclusion chromatography (See Note 4).

3.8 Lipidic Cubic Phase Formation [40–43]

1. Take out monoolein from the freezer and melt it using a heating block at ~40 °C. It takes ~10 min.
2. Remove needles, Teflon ferrules, and plungers from the two 100 μl Hamilton gas-tight syringes (Fig. 4a).
3. Centrifuge the purified membrane protein solution in a 1.5 ml tube at 20,400 g for ~10 min at 4 °C to remove aggregates and collect the supernatant.
4. Check the volume of the supernatant at step 3.

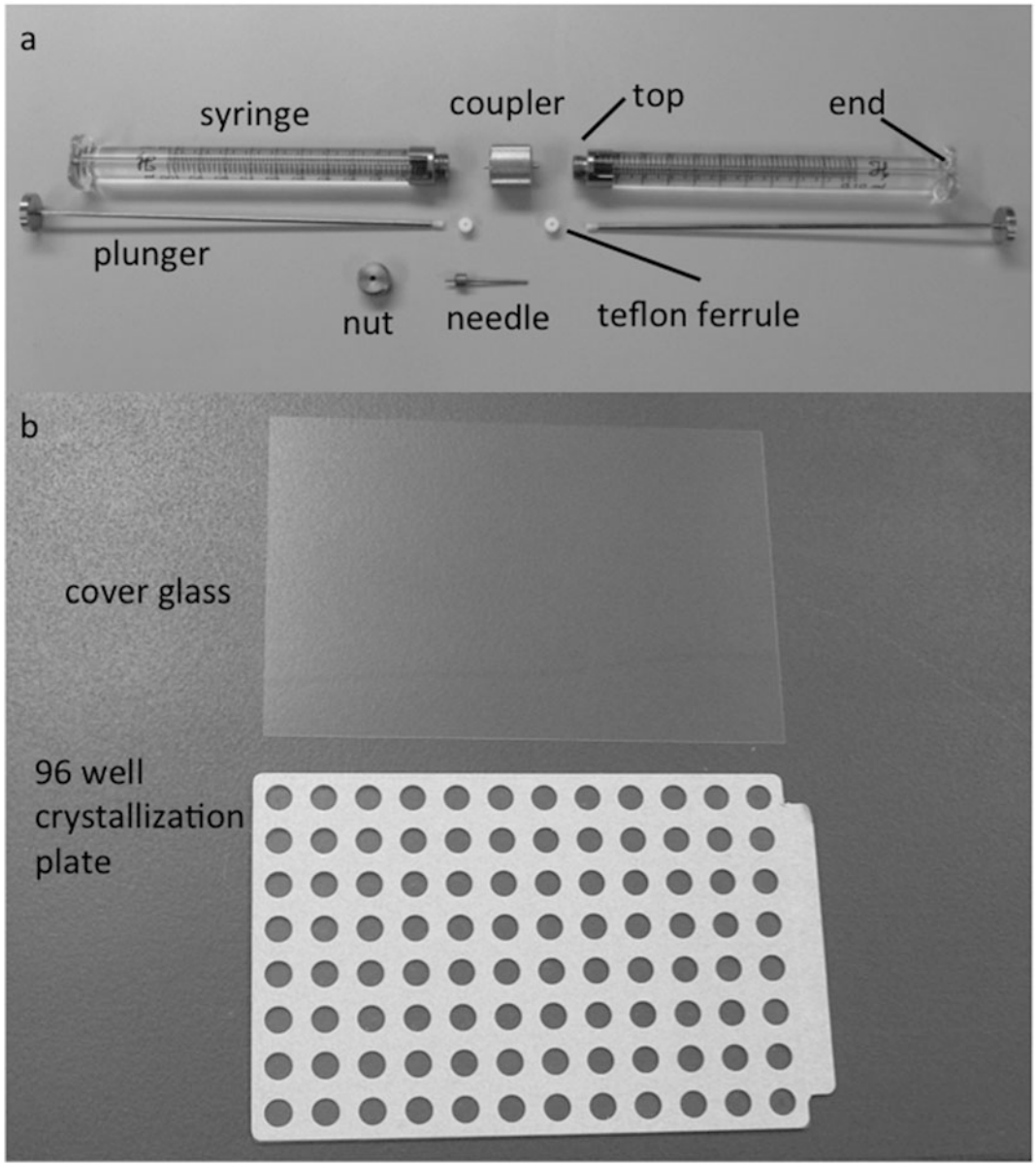

Fig. 4 Apparatus for LCP crystallization. (**a**) Two syringes, two plungers, two teflon ferrules, a coupler, a needle and a nut. (**b**) A cover glass and a 96 well crystallization plate

5. Calculate the required amount of monoolein. The volume of monoolein needs to be ~150 % of the protein solution volume to form the cubic phase (see Note 5).
6. Using a 20 μl or 100 μl pipette and the appropriate disposable tip, put the required amount of melted monoolein into one Hamilton gas-tight syringe from the bottom end (Fig. 4a).
7. Insert a plunger from the bottom end of the syringe. The Teflon part of the plunger will contact with the monoolein.

8. Hold the syringe vertically and push the plunger till monoolein reaches the top end of the syringe. This manipulation will remove air bubbles from the lipid.
9. Using a 20 μl or 100 μl pipette and the appropriate disposable tip, put the membrane protein solution into the other Hamilton gas-tight syringe from the bottom end. Be careful not to trap air bubbles, although air bubbles appear easily because the protein solution contains detergents.
10. Insert a plunger from the bottom of the syringe. The Teflon part of the plunger will contact with protein solution.
11. Hold the syringe vertically and push the plunger until the protein solution reaches the top end of the syringe. If air bubbles are trapped in the solution, remove them by moving the plunger up and down. If this fails, collect the protein solution from the syringe and centrifuge it to remove air bubbles and start again from step 9.
12. Place the Teflon ferrules in the syringes.
13. Connect two syringes by a coupler (Fig. 5a, b).
14. Push slowly the plunger of the syringe that stores the protein solution and transfer all the protein solution into the other

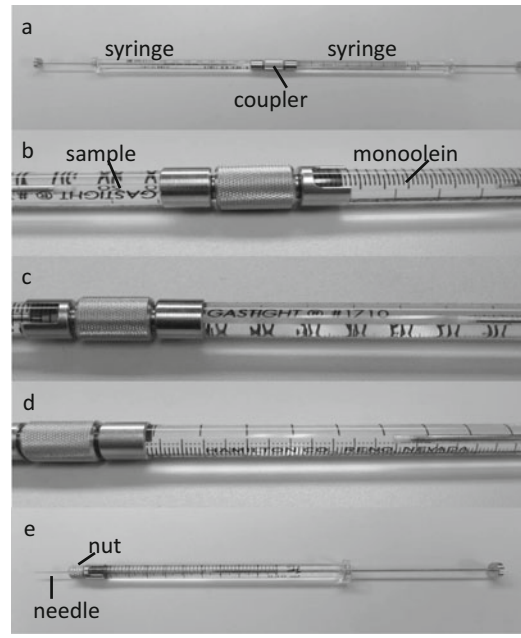

Fig. 5 Outline of the LCP formation. (**a**) Connect two syringes using a coupler. (**b**) One syringe has sample solution and the other has monoolein. (**c**) When mixed, the mixture is clouded. (**d**) Homogeneous cubic phase. (**e**) The syringe with a needle ready for crystallization

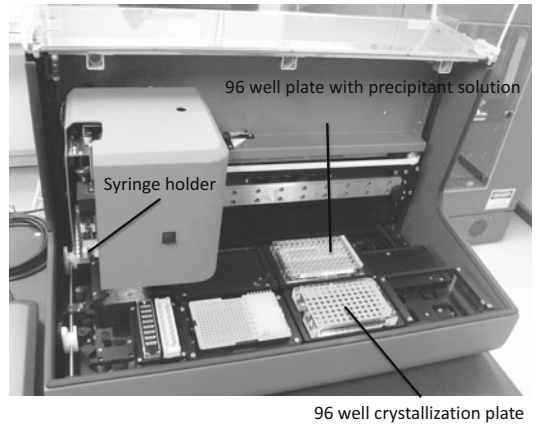

Fig. 6 LCP crystallization robot

syringe through the coupler. This will form a partly clouded mixture (Fig. 5c). Steps 14–16 should be performed at 20 °C.

15. Slowly push the plunger of the syringe that stores the protein solution and monoolein, and transfer them into the other syringe through the coupler.
16. Repeat moving the plungers back and force more than 100 times till the mixture forms a transparent homogeneous cubic phase (Fig. 5d) (See Note 6).

3.9 Crystallization [40–43]

1. Transfer the mixture to one of the two syringes.
2. Disconnect the coupler with the empty syringe from the syringe but keep the Teflon ferrule.
3. Set a needle at the top end of the syringe (Fig. 5e).
4. Place the syringe in the syringe holder of a LCP robot (Fig. 6).
5. Put the 96-well crystallization plate (Fig. 4b) and the 96-well plate containing precipitant solutions in their proper positions on the robot (Fig. 6) (See Note 7).
6. Start the robot. Control the humidity using a humidifier. The volumes of the mesophase and the precipitant solution should be set at 30–50 nl and ~800 nl, respectively.
7. When the robot finishes dispensing, place a cover glass on the crystallization plate (Fig. 4b).
8. Keep the plate in a 20 °C incubator.
9. Check all wells in the plate regularly under a microscope. Use crossed-polarizers as well as normal light. Typically crystals appear in a week, although it may range from a few hours to 2 months (Fig. 7).

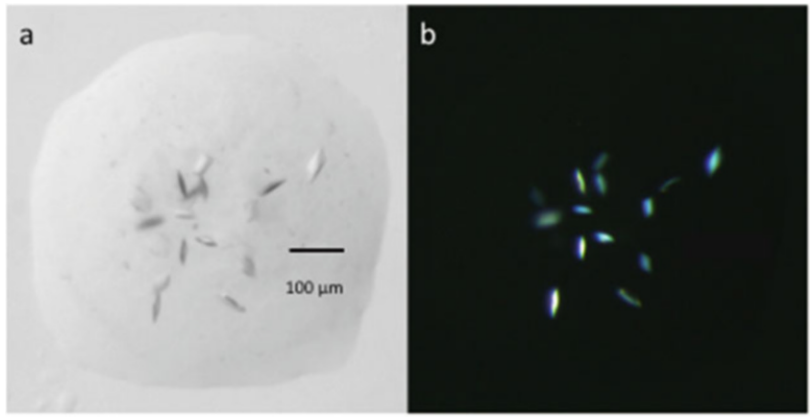

Fig. 7 Crystals of a membrane protein in LCP. Crystals were observed using normal light (**a**) or cross polarizers (**b**)

4 Notes

1. Sonication does not work for the disruption of yeast cells because the cell wall of yeast is harder than bacteria.
2. If an inhibitor, a substrate, or a ligand of the target protein is available, it is advisable to add that compound in the buffers used in the purification steps because the compound will stabilize the protein in a certain conformation and increase the possibility of crystallization.
3. After the TEV protease digestion, the target protein has no His-tag and comes to the flow-through fraction.
4. Purity is less important for the LCP method because LCP can act as a size filter and remove large-size contaminants and protein aggregates [34, 47].
5. For example, if the volume of the membrane protein solution is 20 µl, the volume of monoolein should be 30 µl. Note that monoolein has a density of 0.942 g/ml at 20 °C [48].
6. The recommended rate of mixing is ~1 stroke per second or slower. Faster mixing can raise the temperature of the mixture due to frictional heating which destabilizes the protein.
7. Homemade screens are used. Typically, precipitant solutions contain 30 ~40 % low-molecular-weight PEG (PEG200, PEG300, PEG400, PEG600, PEG500MME, PEG500DME etc.), salts, and buffer at pH 6–8. Note that monoolein is unstable at lower or higher pH.

Acknowledgments

This work was supported partly by JSPS KAKENHI Grant Numbers 26102725 and 15H04338.

References

1. Almen MS, Nordstrom KJ, Fredriksson R, Schioth HB (2009) Mapping the human membrane proteome: a majority of the human membrane proteins can be classified according to function and evolutionary origin. BMC Biol 7:50. doi:10.1186/1741-7007-7-50
2. Fagerberg L, Jonasson K, von Heijne G, Uhlen M, Berglund L (2010) Prediction of the human membrane proteome. Proteomics 10 (6):1141–1149. doi:10.1002/pmic.200900258
3. http://www.rcsb.org/
4. http://blanco.biomol.uci.edu/mpstruc/
5. Iwata S (2003) Methods and results in crystallization of membrane proteins. Internat'l University Line, La Jolla
6. Carola Hunte GJ, Schägger H (2003) Membrane protein purification and crystallization, a practical guide. Academic Press, San Diego
7. Garavito RM, Ferguson-Miller S (2001) Detergents as tools in membrane biochemistry. J Biol Chem 276(35):32403–32406. doi:10.1074/Jbc.R100031200
8. Chae PS, Rasmussen SGF, Rana RR, Gotfryd K, Chandra R, Goren MA, Kruse AC, Nurva S, Loland CJ, Pierre Y, Drew D, Popot JL, Picot D, Fox BG, Guan L, Gether U, Byrne B, Kobilka B, Gellman SH (2010) Maltose-neopentyl glycol (MNG) amphiphiles for solubilization, stabilization and crystallization of membrane proteins. Nat Methods 7 (12):1003–U1090. doi:10.1038/Nmeth.1526
9. Rasmussen SGF, DeVree BT, Zou YZ, Kruse AC, Chung KY, Kobilka TS, Thian FS, Chae PS, Pardon E, Calinski D, Mathiesen JM, Shah STA, Lyons JA, Caffrey M, Gellman SH, Steyaert J, Skiniotis G, Weis WI, Sunahara RK, Kobilka BK (2011) Crystal structure of the beta(2) adrenergic receptor-Gs protein complex. Nature 477(7366):549–U311. doi:10.1038/Nature10361
10. Kruse AC, Hu JX, Pan AC, Arlow DH, Rosenbaum DM, Rosemond E, Green HF, Liu T, Chae PS, Dror RO, Shaw DE, Weis WI, Wess J, Kobilka BK (2012) Structure and dynamics of the M3 muscarinic acetylcholine receptor. Nature 482(7386):552–556. doi:10.1038/Nature10867
11. Rollauer SE, Tarry MJ, Graham JE, Jaaskelainen M, Jager F, Johnson S, Krehenbrink M, Liu SM, Lukey MJ, Marcoux J, McDowell MA, Rodriguez F, Roversi P, Stansfeld PJ, Robinson CV, Sansom MS, Palmer T, Hogbom M, Berks BC, Lea SM (2012) Structure of the TatC core of the twin-arginine protein transport system. Nature 492(7428):210–214. doi:10.1038/nature11683
12. Hemdan ES, Porath J (1985) Development of immobilized metal affinity-chromatography. 2. Interaction of amino-acids with immobilized nickel iminodiacetate. J Chromatogr 323 (2):255–264. doi:10.1016/S0021-9673(01)90388-7
13. Hemdan ES, Porath J (1985) Development of immobilized metal affinity-chromatography. 3. Interaction of oligopeptides with immobilized nickel iminodiacetate. J Chromatogr 323 (2):265–272. doi:10.1016/S0021-9673(01)90389-9
14. Mohanty AK, Simmons CR, Wiener MC (2003) Inhibition of tobacco etch virus protease activity by detergents. Protein Expr Purif 27(1):109–114. doi:Pii S1046-5928(02)00589-2. doi:10.1016/S1046-5928(02)00589-2
15. Hunte C, Richers S (2008) Lipids and membrane protein structures. Curr Opin Struct Biol 18(4):406–411. doi:10.1016/j.sbi.2008.03.008
16. Weyand S, Shimamura T, Yajima S, Suzuki S, Mirza O, Krusong K, Carpenter EP, Rutherford NG, Hadden JM, O'Reilly J, Ma P, Saidijam M, Patching SG, Hope RJ, Norbertczak HT, Roach PCJ, Iwata S, Henderson PJF, Cameron AD (2008) Structure and molecular mechanism of a nucleobase-cation-symport-1 family transporter. Science 322 (5902):709–713. doi:10.1126/Science.1164440
17. Shimamura T, Yajima S, Suzuki S, Rutherford NG, O'Reilly J, Henderson PJF, Iwata S (2008) Crystallization of the hydantoin transporter Mhp1 from microbacterium liquefaciens. Acta Crystallogr F 64:1172–1174. doi:10.1107/S1744309108036920
18. Shimamura T, Weyand S, Beckstein O, Rutherford NG, Hadden JM, Sharples D, Sansom

MSP, Iwata S, Henderson PJF, Cameron AD (2010) Molecular basis of alternating access membrane transport by the sodium-hydantoin transporter Mhp1. Science 328 (5977):470–473. doi:10.1126/Science.1186303

19. Warne T, Serrano-Vega MJ, Baker JG, Moukhametzianov R, Edwards PC, Henderson R, Leslie AG, Tate CG, Schertler GF (2008) Structure of a beta(1)-adrenergic G-protein-coupled receptor. Nature 454(7203):486–491
20. Gast P, Hemelrijk P, Hoff AJ (1994) Determination of the number of detergent molecules associated with the reaction-center protein isolated from the photosynthetic bacterium rhodopseudomonas-viridis – effects of the amphiphilic molecule 1,2,3-heptanetriol. FEBS Lett 337(1):39–42. doi:10.1016/0014-5793(94)80625-X
21. Sennhauser G, Amstutz P, Briand C, Storchenegger O, Grutter MG (2007) Drug export pathway of multidrug exporter AcrB revealed by DARPin inhibitors. PLoS Biol 5 (1):106–113. doi:10.1371/journal.pbio.0050007, ARTN e7
22. Lu M, Symersky J, Radchenko M, Koide A, Guo Y, Nie RX, Koide S (2013) Structures of a Na+-coupled, substrate-bound MATE multidrug transporter. Proc Natl Acad Sci U S A 110 (6):2099–2104. doi:10.1073/Pnas.1219901110
23. Iwata S, Ostermeier C, Ludwig B, Michel H (1995) Structure at 2.8-Angstrom resolution of cytochrome-C-oxidase from paracoccus-denitrificans. Nature 376(6542):660–669. doi:10.1038/376660a0
24. Ostermeier C, Iwata S, Ludwig B, Michel H (1995) F-V fragment mediated crystallization of the membrane-protein bacterial cytochrome-C-oxidase. Nat Struct Biol 2 (10):842–846. doi:10.1038/Nsb1095-842
25. Ostermeier C, Harrenga A, Ermler U, Michel H (1997) Structure at 2.7 angstrom resolution of the Paracoccus denitrificans two-subunit cytochrome c oxidase complexed with an antibody F-V fragment. Proc Natl Acad Sci U S A 94(20):10547–10553. doi:10.1073/Pnas.94.20.10547
26. Hunte C, Koepke J, Lange C, Rossmanith T, Michel H (2000) Structure at 2.3 angstrom resolution of the cytochrome bc(1) complex from the yeast Saccharomyces cerevisiae co-crystallized with an antibody Fv fragment. Struct Fold Des 8(6):669–684. doi:10.1016/S0969-2126(00)00152-0
27. Zhou YF, Morais-Cabral JH, Kaufman A, MacKinnon R (2001) Chemistry of ion coordination and hydration revealed by a K+ channel-Fab complex at 2.0 angstrom resolution. Nature 414(6859):43–48. doi:10.1038/35102009
28. Hino T, Arakawa T, Iwanari H, Yurugi-Kobayashi T, Ikeda-Suno C, Nakada-Nakura Y, Kusano-Arai O, Weyand S, Shimamura T, Nomura N, Cameron AD, Kobayashi T, Hamakubo T, Iwata S, Murata T (2012) G-protein-coupled receptor inactivation by an allosteric inverse-agonist antibody. Nature 482(7384):237–U130. doi:10.1038/Nature10750
29. Rasmussen SG, Choi HJ, Fung JJ, Pardon E, Casarosa P, Chae PS, Devree BT, Rosenbaum DM, Thian FS, Kobilka TS, Schnapp A, Konetzki I, Sunahara RK, Gellman SH, Pautsch A, Steyaert J, Weis WI, Kobilka BK (2011) Structure of a nanobody-stabilized active state of the beta(2) adrenoceptor. Nature 469(7329):175–180. doi:10.1038/nature09648, nature09648 [pii]
30. Kruse AC, Ring AM, Manglik A, Hu J, Hu K, Eitel K, Hubner H, Pardon E, Valant C, Sexton PM, Christopoulos A, Felder CC, Gmeiner P, Steyaert J, Weis WI, Garcia KC, Wess J, Kobilka BK (2013) Activation and allosteric modulation of a muscarinic acetylcholine receptor. Nature 504(7478):101–106. doi:10.1038/nature12735
31. Landau EM, Rosenbusch JP (1996) Lipidic cubic phases: a novel concept for the crystallization of membrane proteins. Proc Natl Acad Sci U S A 93(25):14532–14535. doi:10.1073/Pnas.93.25.14532
32. Liu W, Hanson MA, Stevens RC, Cherezov V (2010) LCP-Tm: an assay to measure and understand stability of membrane proteins in a membrane environment. Biophys J 98 (8):1539–1548. doi:10.1016/j.bpj.2009.12.4296, S0006-3495(09)06148-7 [pii]
33. Caffrey M (2009) Crystallizing membrane proteins for structure determination: use of lipidic mesophases. Annu Rev Biophys 38:29–51. doi:10.1146/Annurev.Biophys.050708.133655
34. Cherezov V (2011) Lipidic cubic phase technologies for membrane protein structural studies. Curr Opin Struct Biol 21(4):559–566. doi:10.1016/J.Sbi.2011.06.007
35. Wadsten P, Wohri AB, Snijder A, Katona G, Gardiner AT, Cogdell RJ, Neutze R, Engstrom S (2006) Lipidic sponge phase crystallization of membrane proteins. J Mol Biol 364(1):44–53. doi:10.1016/J.Jmb.2006.06.043
36. Cherezov V, Clogston J, Papiz MZ, Caffrey M (2006) Room to move: crystallizing membrane

proteins in swollen lipidic mesophases. J Mol Biol 357(5):1605–1618. doi:S0022-2836(06)00078-7 [pii] 10.1016/j.jmb.2006.01.049

37. Shiroishi M, Kobayashi T, Ogasawara S, Tsujimoto H, Ikeda-Suno C, Iwata S, Shimamura T (2011) Production of the stable human histamine H(1) receptor in Pichia pastoris for structural determination. Methods 55(4):281–286. doi:10.1016/j.ymeth.2011.08.015
38. Shimamura T, Shiroishi M, Weyand S, Tsujimoto H, Winter G, Katritch V, Abagyan R, Cherezov V, Liu W, Han GW, Kobayashi T, Stevens RC, Iwata S (2011) Structure of the human histamine H1 receptor complex with doxepin. Nature 475(7354):65–70. doi:10.1038/nature10236. nature10236 [pii]
39. Newby ZER, O'Connell JD, Gruswitz F, Hays FA, Harries WEC, Harwood IM, Ho JD, Lee JK, Savage DF, Miercke LJW, Stroud RM (2009) A general protocol for the crystallization of membrane proteins for X-ray structural investigation. Nat Protoc 4(5):619–637. doi:10.1038/Nprot.2009.27
40. Caffrey M, Cherezov V (2009) Crystallizing membrane proteins using lipidic mesophases. Nat Protoc 4(5):706–731. doi:10.1038/Nprot.2009.31
41. Cherezov V http://cherezov.usc.edu
42. Caffrey M, Porter C (2010) Crystallizing membrane proteins for structure determination using lipidic mesophases. J Visualized Exp: JoVE (45) e1712. doi:10.3791/1712
43. Liu W, Cherezov V (2011) Crystallization of membrane proteins in lipidic mesophases. J Visualized Exp: JoVE (49) e2501. doi:10.3791/2501
44. QIAGEN (2003) A handbook for high-level expression and purification of 6xHis-tagged proteins. QIAGEN, Hilden
45. TALON Metal Affinity Resins User Manual
46. Affymetrix Anatrace Products catalog
47. Kors CA, Wallace E, Davies DR, Li L, Laible PD, Nollert P (2009) Effects of impurities on membrane-protein crystallization in different systems. Acta Crystallogr D 65:1062–1073. doi:10.1107/S0907444909029163
48. Lide DR (2008) CRC handbook of chemistry and physics, 89th edn. CRC Press, Boca Raton